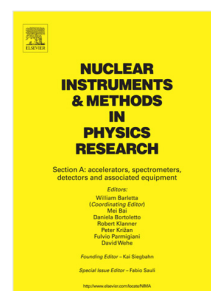


Accepted Manuscript

Single Event Upset tests and failure rate estimation for a front-end ASIC adopted in high-flux-particle therapy applications

F. Fausti, G. Mazza, S. Giordanengo, O.H. Ali, L. Manganaro, V. Monaco, R. Sacchi, R. Cirio



PII: S0168-9002(18)31758-3
DOI: <https://doi.org/10.1016/j.nima.2018.11.106>
Reference: NIMA 61647

To appear in: *Nuclear Inst. and Methods in Physics Research, A*

Received date: 1 August 2018
Revised date: 20 November 2018
Accepted date: 21 November 2018

Please cite this article as: F. Fausti, G. Mazza, S. Giordanengo et al., Single Event Upset tests and failure rate estimation for a front-end ASIC adopted in high-flux-particle therapy applications, *Nuclear Inst. and Methods in Physics Research, A* (2018), <https://doi.org/10.1016/j.nima.2018.11.106>

This is a PDF file of an unedited manuscript that has been accepted for publication. As a service to our customers we are providing this early version of the manuscript. The manuscript will undergo copyediting, typesetting, and review of the resulting proof before it is published in its final form. Please note that during the production process errors may be discovered which could affect the content, and all legal disclaimers that apply to the journal pertain.

1 Single Event Upset tests and failure rate estimation for a front-end
 2 ASIC adopted in high-flux-particle therapy applications

3 F. Fausti^{a,b,d}, G. Mazza^b, S. Giordanengo^b, O. H. Ali^{b,c}, L. Mangano^{b,c}, V. Monaco^{b,c},
 4 R. Sacchi^{b,c}, R. Cirio^{b,c}

5 ^a*Politecnico di Torino, Corso Duca degli Abruzzi, 24, 10129 Torino, Italy*

6 ^b*Istituto Nazionale di Fisica Nucleare, sez. di Torino, via P. Giuria, 1, 10125 Torino, Italy*

7 ^c*Università degli studi di Torino, via P. Giuria, 1, 10125 Torino, Italy*

8 ^d*Corresponding author; E-mail address: fausti@to.infn.it*

9 **Abstract**

10 A 64 channels Application Specific Integrated Circuit, named TERA09, designed in a
 11 $0.35\ \mu\text{m}$ technology for particle therapy applications, has been characterized for Single Event
 12 Upset probability. TERA09 is a current-to-frequency converter that offers a wide input
 13 range, extending from few nA to hundreds of μA with linearity deviations in the order
 14 of a few percent. This device operates as front end readout electronics for parallel plate
 15 ionization chambers adopted in clinical applications. This chip is going to be located beside
 16 the monitor chamber, thus not directly exposed to the particle beam. For this reason, no
 17 radiation hardening techniques were adopted during the microelectronics design. The intent
 18 of the test reported in this paper is to predict the TERA09 upset rate probability in a
 19 real application scenario. Due to the fact that TERA09 has an extended digital area with
 20 registers and counters, it is interesting to estimate the effect of the secondary neutron field
 21 produced during the treatment. The radiation damage test took place at the SIRAD facility
 22 of the Italian National Institute for Nuclear Physics in Padova, Italy. The SIRAD facility
 23 allows to study the CMOS upset rate as a function of the energy deposited during irradiation.
 24 By irradiating the chip with ions of different Linear Energy Transfer, it is possible to calculate
 25 the single event effect cross section as a function of the deposited energy. It resulted that
 26 the minimum deposited energy in a CMOS silicon sensitive volume of $1\ \mu\text{m}^3$, responsible for
 27 a Single Event Upset probability higher than zero, is 690 keV. In the last part of the paper,
 28 we calculated the expected upset probability in a typical clinical environment, knowing the
 29 fluence of secondary backward-emitted neutrons. Considering as an example a treatment
 30 room located at the CNAO particle therapy center in Pavia, the expected upset rate for
 31 TERA09 is $\sim 10^{-6}$ event./year. Using a redundant and independent monitor chamber, the
 32 upset probability expected during one detector readout is lower than 10^{-24} , as explained in
 33 the document

34 **Keywords:** Particle therapy, Monitor chamber, ASIC, CMOS radiation damage, SEU.

35 1. Introduction

36 Since many decades parallel plate gas ionization chambers are the most used detectors
 37 in the cure of cancer with particles (protons and carbon ions). In this context, a single large
 38 area electrode is used for particle beam flux measurement whereas segmented electrodes
 39 allows the two-dimensional beam position measurements [1]. Ionization chambers require a
 40 multi-channel front-end electronics converting the charge with high accuracy operating with
 41 no dead-time. The collaboration between the University of Turin and the microelectronics
 42 group of the Italian National Institute for Nuclear Physics (INFN) designed and produced
 43 a family of Application Specific Integrated Circuits (ASIC) called TERA [2]. Tailored for
 44 clinical applications as front-end readout of gas detectors in particle therapy, the TERA chips
 45 are used in several clinical devices both for quality control in radiotherapy (e.g. the MatriXX
 46 detector [3] provided by IBA [4] and the monitor chambers developed by DE.TEC.TOR.
 47 Devices and technologies Torino [5]) and for beam monitoring in particle therapy facilities
 48 [6] [7]. The aging effects of the total ionizing dose were studied exposing the previous version
 49 of the TERA chip to an X-ray source. Results are reported in [8].

50 TERA09 is the last chip designed and characterized [9]. In this paper, the results of a Single
 51 Event Upset (SEU) test of TERA09 are reported and analyzed. Even though the ASIC is
 52 not going to be directly exposed to the particle beam, secondary neutron produced in the
 53 interaction with the nozzle, may induce temporary upsets which can occur in the digital
 54 circuitry.

55 A common procedure to characterize a CMOS device for SEU, is measuring the occur-
 56 rence of the effect as a function of the energy deposited irradiating the chip with ion beams.
 57 Irradiation with ions of different Linear Energy Transfer (LET) is thus required for varying
 58 the deposited energy. The SIRAD (Silicon RADIation Damage) facility [10], located at the
 59 15 MV Tandem of the Legnaro National Laboratory (LNL) of the INFN, offers the possibil-
 60 ity to select among different ion sources and to change the beam flux and the beam incident
 61 angle on the Device Under Test (DUT). During the test, the DUT is placed inside a vacuum
 62 chamber, thus minimizing scattering and beam slowing which would occur in air.

63 The TERA09 SEU test focused on the identification of bit-flips occurring in the ASIC coun-
 64 ters and registers. From the bit-flip cross-section as a function of the deposited energy, the
 65 failure rate with a given neutron rate and energy spectrum can be predicted. An example
 66 of application to a clinical environment will be presented and discussed.

67 2. Basics of Single Event Effects in CMOS electronics

68 In CMOS technology the reliability of a system to Single Event Effects (SEE), i.e. per-
 69 turbation induced by the energy deposited by single ionizing particles, is an aspect getting
 70 worse (or at least getting more challenging), with the design detail downscaling. In this
 71 field it is common to refer to Single Event Effects (SEE), distinguishing among heavy and
 72 soft damages. Examples of heavy or permanent damages are the Single Event Burnout,
 73 a destructive effect and the Single Event Latch-up (SEL), a short-circuit that can lead to
 74 burnout if not mitigated in time, by turning off the power supply. However this procedure

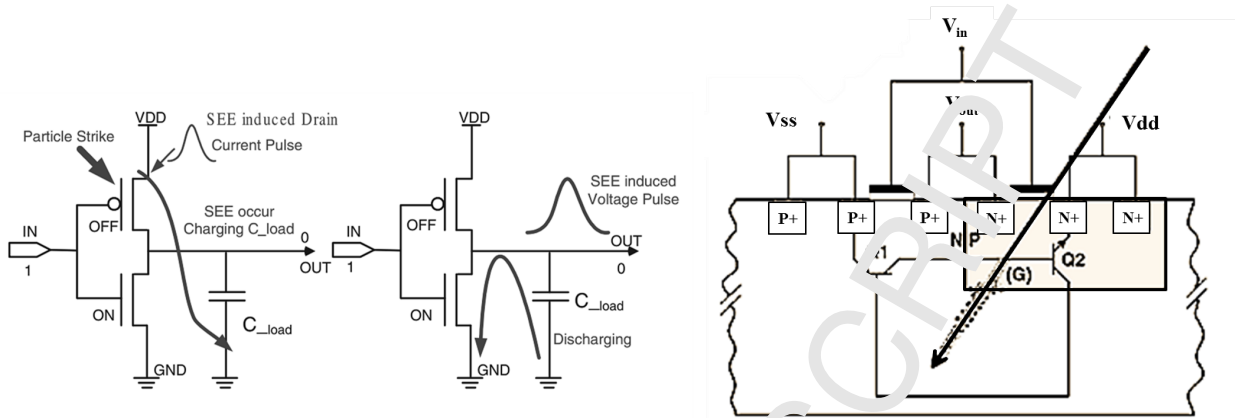


Figure 1: Left: schematic representation of an inverter bit-flip due to a SEE.

Right: The thyristor structure represented with the Q1 and Q2 bipolar transistors path. During a latch-up, both the BJTs are conducting resulting in a short circuit.

75 introduces some dead-time that could affect the data acquisition and should be considered
 76 as SEL consequence. In the soft event category, the Single Event Transient and the Single
 77 Event Upset (SEU) are the most common; the former results in a charge transient caused
 78 by a single proton or heavy ion passing through a sensitive node in the circuit whereas the
 79 latter results in a bit-flip, a logic state change due to energy deposition in a digital cell.
 80 Several studies proved that SEU and SET effects are physically separated in terms of silicon
 81 region where they occur. SEUs are confined in the first micrometers thickness under the
 82 device surface whereas SELs occur deeper in the silicon bulk [11].

83 Single Event Latch-up occurs in deep volume of the the silicon bulk where, in a CMOS
 84 process, the combination of n-well, p-well and substrate forms a parasitic n-p-n-p structure
 85 called a thyristor (see Figure 1 right). During a latch-up both the BJTs are conducting,
 86 resulting in a short circuit, highlighted by the power supply compliance (activation of the
 87 current limitation circuitry). The permanent and destructive event is avoided turning off
 88 the power supply.

89 Single Event Upset in CMOS circuits can be important when exposed to high LET parti-
 90 cles, due to the high released energy in the crossed medium. Hitting the silicon bulk, these
 91 ions create electron-hole pairs and their collection at the source/drain diffusion regions may
 92 result in a p-n junction current pulse, driving a voltage change in that node [12]. More in
 93 detail, in a CMOS structure a SEU happens if an ion strikes the channel region of a NMOS
 94 that is in its off state or if the ion strikes the drain region of an off PMOS. Considering
 95 the general notation of SEE, the event occurs whenever in a sensitive node the charge in-
 96 jected by the current pulse exceeds a given threshold value, represented as a critical charge
 97 Q_{crit} . In the left side of Figure 1 is shown an example of logic state switching occurring
 98 in a CMOS inverter. Considering the "1" logic state at the inverter input node, a charged
 99 particle striking the drain of the PMOS transistor induces a signal at its source; this signal
 100 charges the load capacitance. The discharge of this load capacitance results into an output
 101 voltage pulse (V_{out}), leading to a state-flip at the inverter cell output node. Considering the

102 TERA09 chip and its application, the study has been focused only on the SEU phenomena.

103

104 It is possible to model the SEU phenomenon with the following equation:

$$V_{out} \geq \frac{Q_{crit}}{C_{load}} = \frac{1}{C_{load}} \int_0^{t_{sw}} i_{ds} dt \quad (1)$$

105 where C_{load} is the load capacitance of the discharging path and t_{sw} is the time delay
 106 between the particle strike and the logic state change (voltage exceeding a certain threshold
 107 value). The drain-source current (i_{ds}) flows into the transistor of the SEU relevant node.

108 3. The Device Under Test

109 TERA09 is a 64 channels ASIC designed in a $0.35 \mu\text{m}$ process and taped-out in an
 110 Europractice multi-project wafer (the ASIC extended description and characterization is
 111 reported in [9]). This chip operates as the front-end readout electronics for ionization
 112 chambers and is designed for high-intensity ion-beams. The TERA09 has bipolar inputs,
 113 with a positive and a negative threshold control: once one threshold is crossed, a pulser
 114 block sends a charge quantum to the amplifier input. In this manner, the ASIC converts
 115 the analog information provided by the current integrated over the feedback capacitance of
 116 a differential folded cascode amplifier into the rate of charge quanta subtracted or added to
 117 this capacitance, according to the input signal polarity. This sequence is controlled by means
 118 of a finite state machine requiring four clock cycles and it avoids the amplifier saturation,
 119 thus obtaining a dead time free front-end. The high dynamic range of TERA09, allows a
 120 linear conversion in the range $3 \text{ nA} - 150 \mu\text{A}$, with a linearity deviation smaller than 4%.

121 The TERA09 block diagram representation is presented in Figure 2. The 64 identical
 122 independent input channels are fed into a current to frequency converter representing the
 123 front-end logic which is followed by a 32-bit counter and register; the data transfer between
 124 the former and the latter is activated with a digital load signal without adding a dead time,
 125 independently from the signal conversion operations. TERA09 integrates an adder tree,
 126 activated by the same load signal mentioned before and providing the sum of groups of 4,
 127 16 and 64 channels. These values are stored in additional 34-, 36-, and 38-bit wide registers
 128 which can be addressed via seven digital Channel Select lines and read out on a 38-bit out-
 129 put bus through a multiplexer. This system is designed to allow reading directly the sum
 130 of the counters of 4, 16 or 64 channels if, in order to increase the dynamic range, the input
 131 current is split among these channels. A total of 2774 data bit storage, arranged in 85 data
 132 registers, covers a sizable area of the chip and may suffer data corruption, once the ASIC is
 133 exposed to external radiation.

134

135

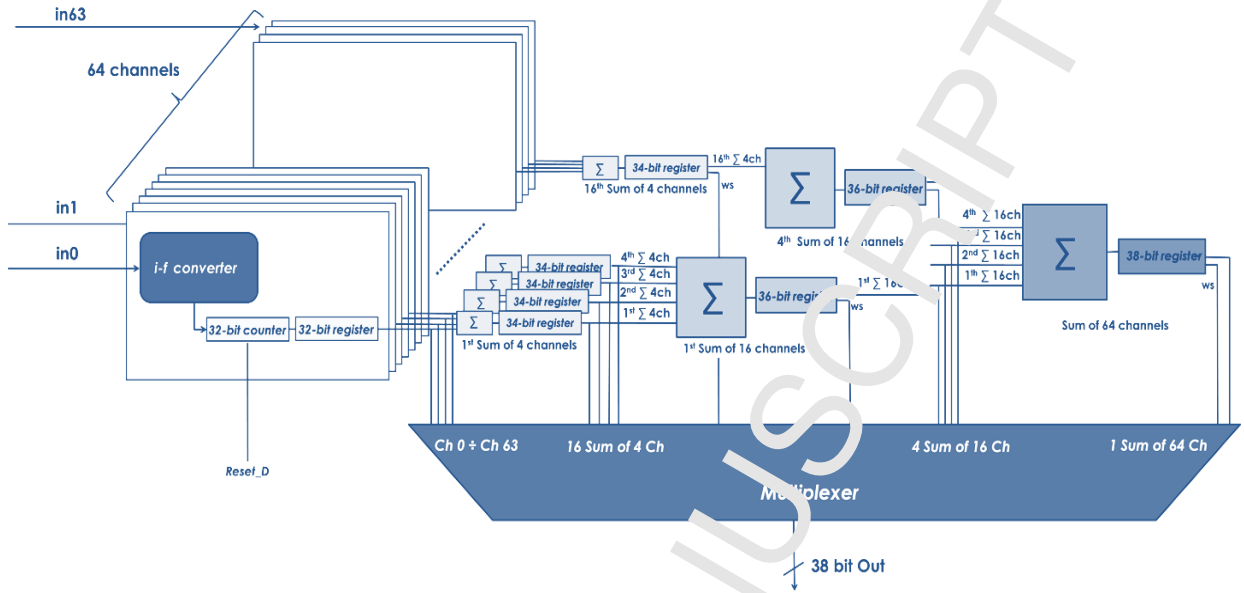


Figure 2: Block diagram of the TERA09 ASIC.

136 4. Test setup

137 The SEU phenomenon results as a bit flip originated by a high energy deposition of a
 138 single track in a small sensitive volume located into the digital circuitry. To study this effect
 139 in a controlled scenario, the particle flux rate must be carefully selected to be low enough
 140 to distinguish the effects caused by the impacts of single ions and high enough to observe
 141 a significant number of single effects in the measurement time. Typical ion fluence rate
 142 are in a range from 10^3 to 10^5 $\text{ions} \cdot \text{m}^{-2} \cdot \text{s}^{-1}$ [10]. The experimental setup set for the
 143 SEU test consists of the TERA09, the device under test placed into a socket soldered on
 144 a PCB test board that interface the ASIC to the Data Acquisition System (DAQ), based
 145 on a Xilinx 7813R FPGA board configured through host PC with the LabVIEW for FPGA
 146 software toolkit. A voltage generator supplied the PCB 5V voltage, with a current limiter
 147 set to protect from burn-out due to a latch-up. The ASIC 250 MHz clock was provided
 148 externally with a LVDS signal source. The main goal of the DAQ software is checking how
 149 many times any bit of the 85 registers changes, due to upset events. In order to do that, the
 150 load signal used to transfer the data from the counter to the registers, was fixed as inactive,
 151 after a first trial acquisition run. A Keithley 2400 voltage generator was used to provide a
 152 steady current to the 64 inputs of the chip in order to let the counters increment rapidly
 153 after the power-up of the chip. This was necessary considering that upsets leading to a 0-1
 154 bit and 1-0 transitions could occur with different probabilities and we wanted to measure
 155 the upset rate in a condition where zeros and ones are uniformly distributed in the register
 156 cells. Moreover, the registers content were also saved in a file for off-line analysis.

157 Along the SIRAD beam line, a vacuum chamber contains the metal plate for the DUT

158 holding (Figure 3). The pressure in the vacuum chamber was set to $\sim 8 \cdot 10^{-6}$ mbar [10].

159 The holder is mechanically controlled by the user who can retract the DUT during
 160 the setup of the accelerator and then align it in front of the beam for the measurement.
 161 Moreover, the vacuum chamber is equipped with two sets of silicon diodes, one fixed and
 162 the other one movable (Figure 3). The fixed diodes are located in front of the final beam
 163 collimator and are used to monitor the beam fluence during the irradiation. Before starting
 164 the measurements, the DUT is kept in a retracted position and the beam is centered and
 165 focalized with the aid of a scintillator imaged by a CCD camera. Then, the fixed diodes
 166 are cross-calibrated with the movable silicon diodes which are temporary inserted in the
 167 position where the DUT will be placed during the tests. At the end of the calibration, the
 168 movable diodes were retracted.

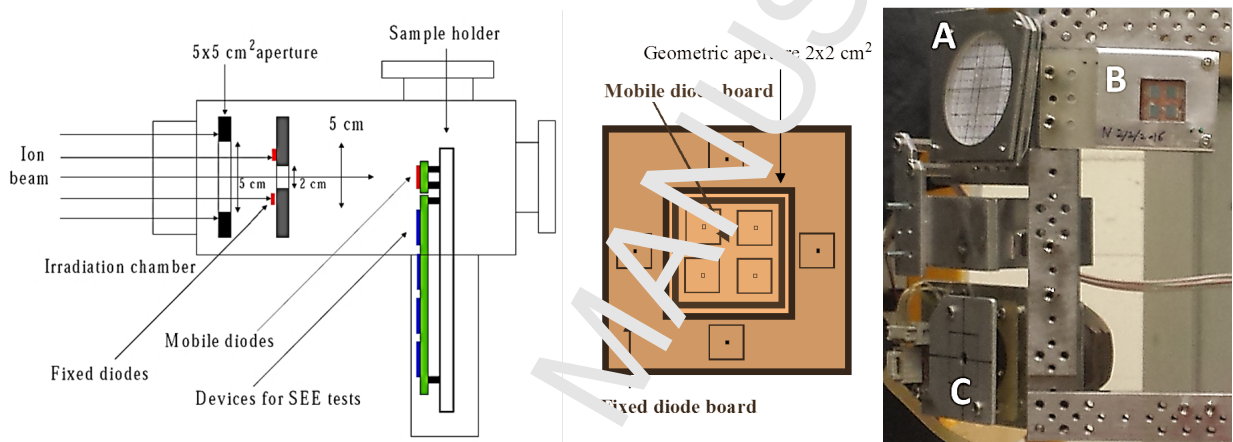


Figure 3: Schematic drawing of the irradiation chamber with the dosimetry system and the device under test holder (left). Diodes geometry and placement scheme (center). Right: vacuum chamber inner picture: A) scintillator; B) fixed diodes; C) movable diodes.

169 The TERA09 ASICs are packaged in a MQFP 160 pins ceramic structure. The chip is
 170 then carried by a plastic socket. In order to expose the $4.68 \times 5.8 \text{ mm}^2$ silicon area of the
 171 chip, the ceramic cover of the package was removed and a hole was drilled in the socket.

172 All the interconnection cables were adapted or customized for the SEU test, in order to
 173 setup the data transfer through the vacuum chamber. The differential clock was provided
 174 via SMA cables. From a control room, outside the accelerator area, a remote desktop was
 175 used to set and control the DAQ and for the on-line monitoring of the raw data. With
 176 the adopted test procedure, the signal that loads the registers with the counters content
 177 was turned off after the initialization phase. At that point, any change in the registers is
 178 considered as originated by bit flips are due to SEUs. An iterative control every 100 ms
 179 checked the 2774 memory bits and a SEU counter was updated every bit-flip occurrence.

180 5. Results and data analysis

181 The SEU test performed with the TERA09 ASIC was devoted to the digital circuitry of
 182 registers. In this case, the focus is on the single bit flip due to a radiation-induced upset.

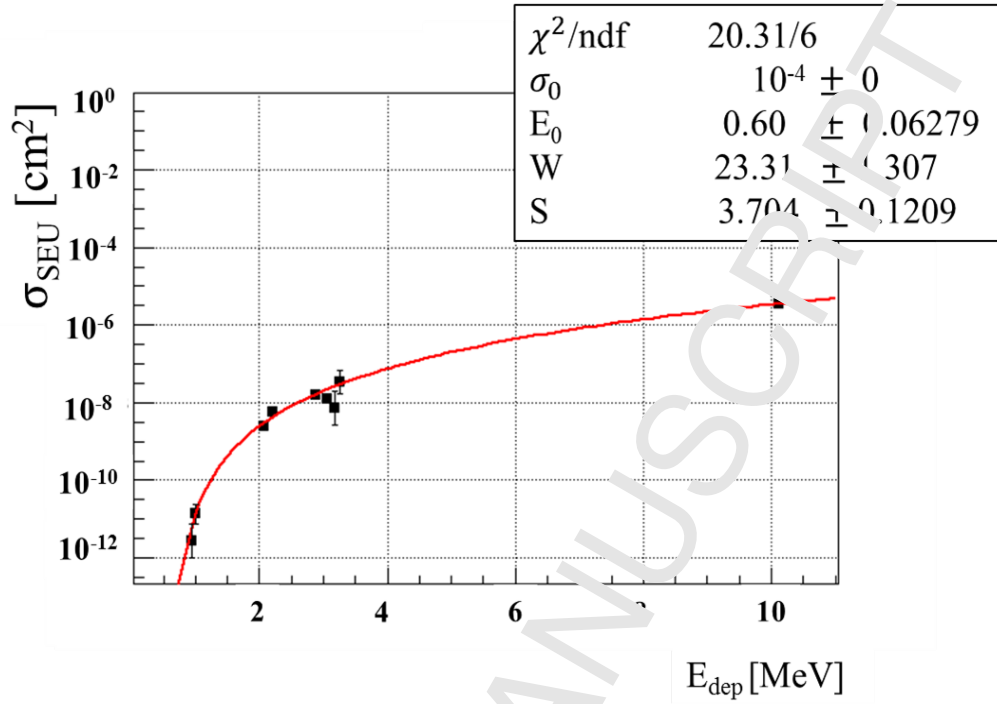


Figure 4: SEU cross-section as a function of the deposited energy.

183 The SEU cross section is defined as:

$$\sigma_{SEU} = \frac{N_{errors}}{\phi N_{bit}} \quad (2)$$

184 and corresponds to the probability per unit fluence and per bit cell of a bit-flip in the
 185 cell. Figure 4 shows the SEU cross section as a function of the deposited energy E_{dep} . The
 186 conversion from LET to E_{dep} was made according to [13].

187 As suggested by the approach described in [11], the Weibull function is used to fit the SEU
 188 cross section as a function of the deposited energy. The trend followed by this function
 189 describes those phenomena starting with a threshold activation mechanism and saturating
 190 at large values. The same method takes into account a $1 \times 1 \times 1 \mu\text{m}^3$ Sensitive Volume (SV)
 191 as the elementary reference volume where a SEU can occur. In SEU studies, E_0 is the the
 192 minimum energy that has to be deposited in the sensitive volume to trigger the upset event;
 193 the saturation level is the maximum SEU cross-section, due to the fact that each sensitive
 194 area is already affected by an upset. In a simple geometrical model, σ_0 should correspond
 195 to the effective sensitive area for SEU phenomena.

196 The Weibull function is:

$$\sigma_{SEU} = \sigma_0 [1 - e^{-(E_{dep} - E_0/W)^s}] \quad (3)$$

197 where E_{DEP} is the energy deposited in the silicon; s and W are fit parameters.

Table 1: List of used ions and the corresponding energy, DUT-particle beam angle, deposited energy and cross section.

Ion	Energy [MeV/u]	Angle [°]	Edep [MeV]	σ_{SEU}
^{19}F	122	0	0.94	$2.73e^{-12}$
^{19}F	122	20	1.00	$1.34e^{-11}$
^{28}Si	157	0	2.08	$2.554e^{-09}$
^{28}Si	157	20	2.21	$5.33e^{-09}$
^{35}Cl	171	0	3.07	$1.88e^{-09}$
^{35}Cl	171	15	3.18	$7.10e^{-09}$
^{35}Cl	197	0	2.87	$1.53e^{-08}$
^{35}Cl	197	20	3.06	$1.21e^{-08}$
^{79}Br	241	0	10.12	$3.6e^{-06}$

198 The ions used for the TERA09 SEU test are reported in Table 1. The choice of the ion set
 199 was made considering that one needs data for both the threshold region and the saturation
 200 plateau. For ions with high LET the measurement was affected by latch-up events in the
 201 silicon bulk. In these cases, the current limitation of the voltage supply avoided short-circuit
 202 destructive consequences. Using a bromine ion beam, corresponding to deposited energy of
 203 10.12 MeV, the data acquisition was interrupted by frequent latch-up just after few seconds,
 204 thus allowing the acquisition of very short runs. No SEL events were observed with chlorine
 205 beam. As explained in the following section, given the relatively large deposited energy
 206 for the onset of SEL, no occurrence is expected in a clinical environment and no further
 207 investigations were attempted to determine the SEL cross-section. In addition, with ions
 208 lighter than fluorine, no SEU were observed. Changing the incident angle between beam and
 209 DTU allowed to slightly increase the deposited energy and to add a second energy-deposited
 210 point, for the same ion.

211

212 6. Expected SEU rate in a clinical room

213 The TERA09 ASIC follows the family of devices developed by our group that are equip-
 214 ping clinical monitor chambers worldwide. The previous versions of these chips, named
 215 TERA06 and TERA08 are routinely used in particle therapy centers like the National Cen-
 216 ter for Oncological Hadron therapy (CNAO) [7] in Pavia, where our group has a consolidated
 217 role of research and technological collaboration since the center foundation. Since TERA09
 218 has a more extended digital circuitry, compared to its predecessors, it is interesting to es-
 219 timate the upset rate for TERA09 in a CNAO treatment room. The results of this study
 220 are hereafter reported. CNAO has a 25 m diameter synchrotron that accelerates protons
 221 and carbon ions in the energy range of 60 MeV - 250 MeV and 120 MeV/u - 400 MeV/u
 222 respectively. In the monitor chambers, the TERA ASICs are placed beside the gas volume
 223 and are not directly exposed to the proton beam flux; in this situation, the only source of
 224 upset events would be the secondary neutrons, backward emitted at the beam extraction

225 point.

226 This hypothesis is supported by the data of Table 2 and the results reported in the same
 227 paper [14], where FLUKA Monte Carlo simulations show that the largest contribution that
 228 could be relevant for the radiation damage to the readout electronics are the secondary
 229 neutrons backward emitted by the interaction between the 400 MeV/u carbon ions and the
 230 target.

Table 2: Number of secondary neutrons and protons produced by carbon ion and proton beams on ICRU tissue (International Commission on Radiation Units and Measurements).

Target	Primary particles	n/primary	p/primary
ICRU tissue	400 MeV/u carbon ions	2.00	1.50
ICRU tissue	120 MeV protons	0.11	0.10

231 In this paper, a $3.4 \cdot 10^{10} \text{ n} \cdot \text{cm}^{-2}$ annual flux of secondary neutrons at the nozzle, where
 232 the monitor chambers are located, was estimated using a 400 MeV/u carbon ion beam.
 233 Experimental data and simple theoretical arguments reported in [11] confirm that the
 234 SEU rate for neutrons and protons with an energy exceeding 20 MeV are expected to be
 235 equivalent. The probabilities per unit flux of ionizing energy deposition larger or equal to
 236 E_{dep} in a sensitive volume were simulated in [11] for four different proton energies, yielding
 237 the results reported in Figure 5.

238 The choice of a sensitive volume of $1 \times 1 \times 1 \text{ } \mu\text{m}^3$ was justified by the authors as the one
 239 best matching the measured SEU cross section over 18 devices analyzed [11]. In a simplified
 240 model where an upset would always occur above an energy threshold, the 20 MeV proton
 241 data of Figure 5 could be interpreted as the SEU cross section in the CNAO environment as
 242 a function of the SEU energy threshold of the electronic device under study. However, since
 243 this simplistic step-like model is not realistic, we significantly improve it by using the results
 244 of the Weibull fit of Figure 4. For each energy bin i , if P_i represents the probability per unit
 245 flux from Figure 5 and A the cross-sectional area of the sensitive volume ($1 \times 1 \text{ } \mu\text{m}^2$),
 246 the quantity P_i/A represents the probability for a particle crossing the area A of depositing
 247 an energy larger or equal to E_i . This probability has to be weighted by the increase in the
 248 SEU cross section in that same energy interval can be evaluated from the Weibull fit as
 249 $(\sigma_{i+1} - \sigma_i)$. Therefore, the SEU cross section Σ in the neutron environment of CNAO can
 250 be derived as

$$\Sigma = \sum_i P_i \cdot (\sigma_{i+1} - \sigma_i) / A \quad (4)$$

251 Assuming the neutron flux reported in [14] and considering a similar energy deposition
 252 probability as a 20 MeV proton beam, the SEU rate for TERA09 in a CNAO typical clinical
 253 treatment room is $\sim 10^2$ SEU/year. Such an upset would be easily detected, thanks to the
 254 comparison with a second independent detector (as explained in [15]). A SEU would escape
 255 the redundant control only if the data corruption would occur in the same readout cycle
 256 and in the same bit in both detectors.

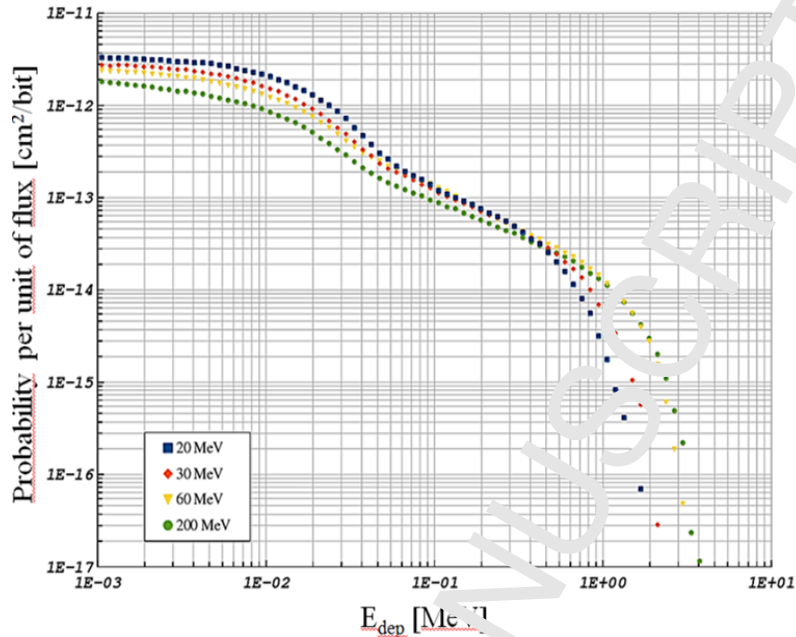


Figure 5: Energy deposition probabilities for protons of different energies. The curves show the probability to have an ionizing deposition greater or equal to the indicated E_{DEP} , within the SV. Data from [11]. The curve selected for the data analysis is the one for 20 MeV protons corresponding to the average value in Figure 6.

257 From a conservative calculation, considering 1 MHz as typical CNAO monitor chamber
 258 readout frequency and a one-year-continuous data acquisition, the probability of failing
 259 the SEU detection in one readout cycle is $\sim 10^{-12}$ for each detector, i.e. $\sim 10^{-24}$ for a
 260 simultaneous upset.

261 Given the even larger deposited energy for the onset of SEL, compared to SEU, latch-up
 262 events are not expected to show-up in clinical applications.

263 7. Summary

264 The TERA09 ASIC is a 34 channels current to frequency converter designed in the 0.35
 265 μm technology, to be employed as front-end readout electronics in particle therapy appli-
 266 cations. The chip does not have embedded radiation protection techniques since it is not
 267 meant to be placed directly on beam during its activity. Nevertheless, the group was in-
 268 terested in characterizing the device for SEU. The test has been performed at the SIRAD
 269 Tandem accelerator at LNL in Padova, using a set of heavy ions with different energies and
 270 and target incidence angles. In this way it was possible to calculate the single event effect
 271 cross-section as a function of the deposited energy. It results that the minimum deposited
 272 energy in a CMOS silicon sensitive volume of $1 \mu\text{m}^3$, responsible for a Single Event Upset
 273 probability higher than zero is 690 keV. Due to the fact that this ASIC will be used in

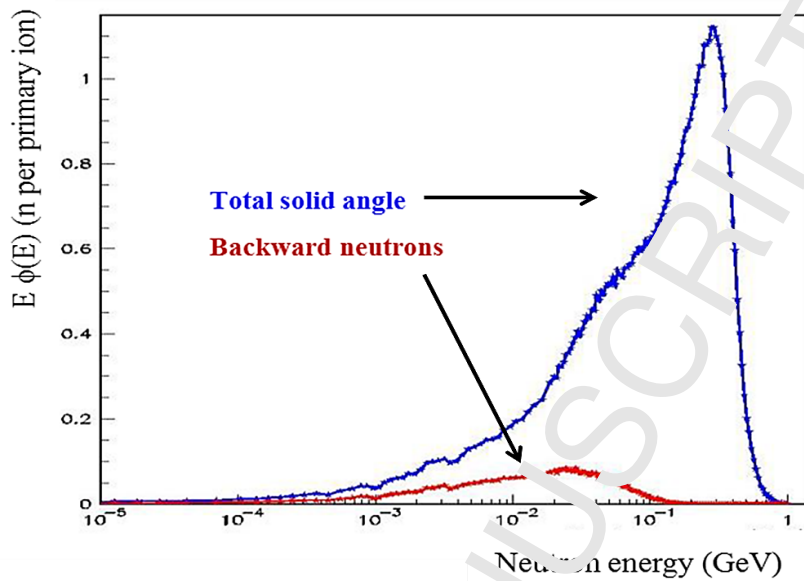


Figure 6: Spectrum of secondary neutrons produced in the backward direction by 400 MeV/u carbon ions, hitting a phantom made of ICRU tissue (International Commission on Radiation Units and Measurements); a comparison is made with the total energy spectrum of secondary neutrons.

274 medical applications, there was an interest in predicting the expected upset rate in a typical
 275 treatment room of CNAO. Assuming the literature data regarding the secondary neutron
 276 fluence at the CNAO nozzle and following the model developed in [11], we derived a num-
 277 ber, $\sim 10^2$ SEU/year, which is an order of magnitude of the phenomenon.
 278 This rate is easily controllable through redundancy, with a second independent monitor
 279 chamber already present at CNAO as in every standard clinical monitor systems. The prob-
 280 ability to have a simultaneous bit flip in the same bit of both the monitor chambers, in a
 281 given detector readout cycle is therefore absolutely negligible (below 10^{-24} SEU/readout-
 282 cycle).

283
 284
 285
 286

287 References

- 288 [1] S. Giordanengo *et al.*, Review of technologies and procedures of clinical dosimetry for scanned ion beam
 289 radiotherapy, *Phys. Medica* 43, (2017) 79–99.
 290 [2] G. Mazza *et al.*, A 64-channel wide dynamic range charge measurement ASIC for strip and pixel ioniza-
 291 tion detector, *Nuclear Science, IEEE Transactions* 52, (2005) 847 – 853.
 292 [3] MatriXX – universal detector array [https://www.iba-dosimetry.com/product/matrixx-universal-](https://www.iba-dosimetry.com/product/matrixx-universal-detector-array/)
 293 [detector-array/](https://www.iba-dosimetry.com/product/matrixx-universal-detector-array/)
 294 [4] <http://www.iba-dosimetry.com/complete-solutions/radiotherapy/quality-assurance/startrack.>
 295 [5] <http://detector-group.com/it/>

- 296 [6] A. La Rosa, *et al.*, Nucl. Instr. Meth. Phys. Res. A 565, (2006) 833.
- 297 [7] S. Giordanengo *et al.*, Design and characterization of the beam monitor detectors of the Italian National
298 Center of Oncological Hadron-therapy (CNAO), Nucl. Instr. Meth. Phys. Res. A 698 (2013), 201-207.
- 299 [8] R. Cirio *et al.*, Radiation damage studies of a recycling integrator VLSI chip for dosimetry and control
300 of therapeutical beams, Nucl. Instr. Meth. Phys. Res. A 482 (2002), 752 – 760.
- 301 [9] F. Fausti *et al.*, Design and characterization of a 64 channels ASIC front-end electronics for high-flux
302 particle beam detectors, Nucl. Instr. Meth. Phys. Res. A, (2017).
- 303 [10] D. Bisello *et al.*, SIRAD: an irradiation facility at the LNL Tandem accelerator for radiation damage
304 studies on semiconductor detectors and electronic devices and systems, Nucl. Instr. Meth. Phys. Res. A
305 462 (2001), 426-434.
- 306 [11] M. Huhtinen, F. Faccio, Computational method to estimate Single Event Upset rates in an accelerator
307 environment, NIM A 450 (2000), 155-172.
- 308 [12] M. Omana *et al.*, A model for transient fault propagation in combinatorial logic, 9th IEEE On-Line
309 Testing Symposium, (2003), 111–115.
- 310 [13] D. G. Mavis *et al.*, SEU and SET modeling and mitigation in deep submicron technologies (2007),
311 IEEE International Reliability Physics Symposium Proceeding, 45th Annual
- 312 [14] A. Ansarinejad *et al.*, Radiation effects on the on-line monitoring system of a hadrontherapy center,
313 Iranian Journal of Medical Physics Vol. 11, No. 4, (2014), 294–300.
- 314 [15] Giordanengo *et al.*, The CNAO Dose Delivery System for ion pencil beam scanning radiotherapy, Medical
315 Physics 42,1 (2015), 263.